DFNE 2014 - 218

Modeling Flow in Naturally Fractured Reservoirs: Effect of Fracture Aperture Distribution on Critical Sub-Network for Flow

J. Gong
Delft University of Technology, Delft, the Netherlands
W. R. Rossen
Delft University of Technology, Delft, the Netherlands

ABSTRACT: Fracture network connectivity and aperture (or conductivity) distribution are two crucial features controlling the flow behavior of fractured formations. The effect of connectivity on flow properties is well documented. We focus here on the influence of fracture aperture distribution. We model a two-dimensional fractured reservoir in which the matrix is impermeable and the fractures are well-connected. The fractures obey a power-law length distribution, as observed in natural fracture networks. For the aperture distribution, since the information from subsurface fracture networks is limited, we test a number of cases: narrow and broad log-normal and power-law distributions, and one where aperture correlates with fracture length. We show that even a well-connected fracture network can behave like a network near the percolation threshold in some cases: i.e., most fractures can be eliminated leaving a critical sub-network with nearly the same permeability as the original fracture network. We determine how broad the aperture distribution must be to approach this behavior, and the dependence of the critical sub-network on the parameters of the aperture distribution. We also explore whether one can identify the critical sub-network without doing flow calculations.

1. INTRODUCTION

A large number of oil and gas reservoirs across the world are naturally fractured, from which significant oil and gas are produced [1]. Reservoirs are recognized as "fractured" primarily if the fractures form an interconnected network. The behavior of a fractured reservoir is very different from that of conventional reservoirs [1-3]. The main reason for this difference is that fractures are far more permeable than matrix: most fluid resides in the matrix blocks, whereas the flow is dominated by the fracture networks. The heterogeneities of fracture networks strongly affect the flow behavior of fractured reservoirs. Field studies and laboratory experiments show flow channeling in individual fractures and highly preferential flow paths in fracture networks [4-6]. Fluid flow is concentrated in a small portion of the fracture network. Cacas *et al* [7, 8] proposed that a broad distribution of fracture conductivity is the main cause of the high degree of flow channeling. In order to understand these phenomena, many theoretical studies have been done. The separate influences of fracture network connectivity [9-22] and fracture conductivity distributions [23-26] on flow channeling have been considered, and also the interplay of these two key factors [27-29]. Particularly, percolation theory is employed in some studies, as it is a powerful mathematical tool to help understanding flow channeling and to capture the preferential flow paths [10-12, 15-17, 19, 23, 27-30]. In addition to the geometrical structure of the conducting network, the effective permeability of network is also a research emphasis [23, 27-30].

Katz and Thompson [31] concluded that if the distribution of pore radii is broad, the permeability of a porous medium is determined mainly by a critical sub-network of widest pores just sufficient to form a percolating cluster. This applies even if the underlying pore network is well-connected, far above the percolation threshold. Similarly, Charlaix [23] modelled fracture networks with broad aperture distributions, and demonstrated that the flow in the sub-network containing fractures with aperture larger than a critical value gives a good approximation of the permeability of the entire network. Berkowitz [32] further pointed out that even a well-connected fracture network can exhibit sparse preferential flow paths if the distribution of fracture conductivities is sufficiently broad.

In this report, we analyze the effect of aperture distribution on the critical sub-network: in other words, how broad the aperture distribution must be that a well-connected fracture network can exhibit a sparse critical sub-network with nearly the same permeability. We believe that in even a well-connected fracture network there can exist a critical sub-network that is a sparse portion of the actual fracture network. Specifically, most of fractures can be removed without significantly affecting the effective permeability of the network.

Fracture network connectivity and fracture aperture distribution are the two key factors which dominate flow behavior in fracture networks. Here we look at well-

connected fracture networks, and our main focus is on the influence of fracture aperture distribution on the critical sub-network carrying most of the flow. As the information on fracture apertures, especially in the subsurface, is limited, we test power-law and log-normal distributions and a case in which aperture is perfectly correlated to fracture length. We examine the effects of aperture distribution on the critical sub-network and its properties.

In section 2 we introduce the numerical model and research process of this study. In section 3 we present the critical sub-network of the fracture network for fracture networks in which fracture aperture follows power-law and log-normal distributions and a case with aperture correlated to fracture length. We use percolation theory to analyze the connectivity of the initial fracture network. In section 4, the possibility of identifying the critical sub-network without doing flow simulations is discussed.

2. NUMERICAL MODEL & RESEARCH PROCESS

2.1 Numerical model

We use the commercial fractured-reservoir simulator FracMan™ [33] to generate the fracture network. A 3D fracture network is generated in a 10 m × 10 m × 0.01 m region. The shape of each fracture is square. Each fracture is perpendicular to the X-Y plane and penetrates the top and bottom boundaries of the region of interest. In this study, the Enhanced Baecher Model is employed to allocate the location of fractures. Two fracture sets, nearly orthogonal to each other, are assumed, with almost equal numbers of fractures in the two sets.

Because of the uncertainties in data and the influence of cut-offs in measurements, fracture trace lengths have been described by exponential, log-normal and power-law distributions in previous studies [34-36]. Currently, a power-law distribution is assumed by many researchers to be the correct model for fracture length [28, 30, 37, 38], with exponents in the range of 1.5 to 3.5. In this study, fracture length follows a power-law distribution (f(x)):

$$f(x) = \frac{\alpha-1}{x_{min}}\left(\frac{x_{min}}{x}\right)^{\alpha} \quad (1)$$

where α is the power law exponent, x is fracture length and x_{min} the lower bound on x, which we take to be 0.6 m. We choose α = 2 and truncate the length distribution on the upper end at 6 m; thus there are no extremely short or long fractures (Fig. 1). In particular, opposite sides of our region of interest cannot be connected by a single fracture. Since even the smallest fracture length (0.6 m) is much larger than the thickness of our region of interest (0.01 m), the 3D model can be seen as a 2D fracture network.

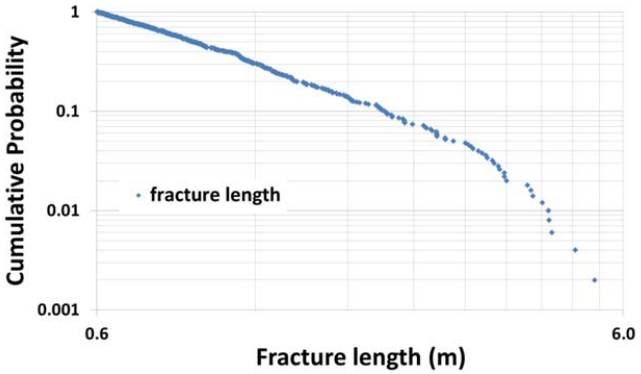

Figure 1 Fracture length follows power-law distribution with exponent α = 2 and minimum and maximum cut-offs of 0.6 and 6 m

For fracture aperture, two kinds of distribution which have been proposed in previous studies are adopted: power-law and log-normal. In each kind of distribution, different parameter values are examined. The aperture is randomly assigned to each fracture. In the cases of aperture perfectly related to fracture length, fracture aperture follows a power-law distribution scaled to fracture length. The details of aperture distribution will be introduced later.

2.2 Flow simulation model

We assume a fracture can be approximated as the slit between a pair of smooth, parallel plates; thus the aperture of each fracture is uniform. Fracture transmissivity is related to aperture by the "cubic law":

$$T = \frac{1}{12}A^3 \quad (2)$$

where A is aperture. We consider steady-state flow through a 10 m × 10 m × 0.01 m fractured rock mass. The matrix is assumed to be impermeable, so that fluid flow can take place only in the fracture network. For computing flow in discrete fracture networks, as in most numerical simulations of flow in fracture networks, Darcy's Law for steady-state incompressible flow is employed, and at each intersection of fractures mass is conserved. In our models, we induce fluid flow from the left side to the right side by applying a constant difference in hydraulic head across the domain while all the other boundaries are impermeable. The equivalent permeability of the fracture network *K* is defined by

$$K = \frac{Q/L\cdot W}{\Delta h/L} \quad (3)$$

where Q is the volumetric flow rate, Δh is the difference in hydraulic head between inflow and outflow boundaries, L is the length of system, and W is the thickness of the region.

We use Mafic™, a companion program of FracMan™, to do the flow simulations.

2.3 Methodology

As mentioned above, our main interest lies in examining the change of equivalent network permeability when a

portion of fractures is eliminated, and the influence of aperture distribution (exponent in a power-law distribution and standard deviation in a log-normal distribution). Countless criteria can be used to decide which portion of fractures to remove, such as fracture length, aperture, length × aperture, velocity, etc. Here we choose a criterion based on the flow simulation results. Mafic^{TM} subdivides the fractures into finite elements for the flow calculations. We obtain the flow velocity at the center of each finite element and the value of flow velocity × aperture (Q_{nodal}). Based on this we compute the average value ($Q_{average}$) of all the elements in each fracture. $Q_{average}$ is then used as the criterion to eliminate fractures: fractures are eliminated in order, starting with the one with smallest value of $Q_{average}$ to the one with the largest $Q_{average}$. In each step, we calculate the flux and the equivalent network permeability for the truncated network. The elimination of fractures is based on flow in the original fracture network, not the truncated network.

We also describe the properties of the "backbone", specifically its length and aperture distribution. Since the matrix is assumed to be impermeable, the fractures which do not belong to the conducting pathways, i.e. the dangling branches or dead ends, can be neglected as they make no contribution to flow. These dead ends are often finite elements within a fracture rather than the entire fracture. The fracture network without these elements is the "backbone". A MATLAB program is used to find the backbone based on the trace map of the fracture network generated by FracMan^{TM}. At the start, and at each step after eliminating fractures based on the initial flow calculation, we further reduce the remaining fracture network to its backbone, by eliminating elements that do not contribute to flow in the cluster.

Because the generation of the fracture network is a random process, an infinite number of fracture networks could be generated with the same parameter values for density, orientation, fracture length and aperture distribution. In this study, for each set of parameter values, we generate one hundred realizations.

2.4 Percolation Theory

Percolation theory is a powerful mathematical tool to analyze transport in complex systems [39]. Percolation theory has been widely used to describe the connectivity and conductivity of fracture networks. The simplest percolation models are site percolation and bond percolation, in which sites or bonds on an infinite lattice are occupied and open to flow with a probability p. To analyze a fracture network, continuum percolation is more applicable, in which fractures can be placed anywhere and can be of variable length. To analyze the connectivity of a fracture network using percolation theory, one must choose a parameter equivalent to the occupancy probability used in site or bond percolation. Different choices have been considered in previous studies. The first is the average number of intersections per fracture [11]. A second is the number of factures in the system [16, 19]. A third is the dimensionless density, defined as $p = Nl^2/L^2$, in which N is the number of fractures, l is the (uniform) fracture length and L is the system size [36]. A fourth choice is the probability that a point is within the effective area of a fracture [40, 41].

As the fracture networks used in this study are generated using the Enhanced Baecher Model, in which the fracture centers are located using a Poisson process, we use the fourth option described above as the percolation parameter p:

$$p = 1 - \exp\left(\frac{-N\langle a_{ex}\rangle}{4L^2}\right) \quad (4)$$

where N is the number of fractures in the system and $\langle a_{ex}\rangle$ is the average excluded area. Excluded area is defined as the area around a fracture in which the center of other fractures cannot lie in order to ensure the fractures do not intersect [42]. For fracture network comprising two orthogonal fracture sets of uniform fracture length l, the average excluded area is $\langle a_{ex}\rangle = l^2/2$ [43]. Masihi *et al* [41] proposed that if a fracture network has a distribution of fracture lengths, its connectivity is identical to that of a system with fixed fracture length equal to the so-called effective length l_{eff}, which is the root-mean-square fracture length:

$$l_{eff}{}^2 = \langle l^2\rangle \ . \quad (5)$$

In this study, percolation theory is employed to analyze the connectivity of the initial fracture network, to illustrate how far above percolation threshold, and how well-connected, the initial fracture network is.

The percolation threshold p_c is the value at which a cluster of fractures connects the opposite sides of the region. The threshold value is affected by the position, orientation, and length distribution of fractures, system size, etc. Masihi *et al* [41] studied the percolation threshold of fracture networks with different fracture length distributions and different system sizes. For fracture networks generated in a 10 m × 10 m region with random orientation, when the length follows a power-law distribution with exponent α = 2, they proposed that the percolation threshold is around 0.66. In our case, the system size and power-law exponent are consistent with their work, but the fractures are not randomly orientated, but in two perpendicular sets. As proposed by Masihi *et al* [40, 41], the percolation threshold for fracture network with two perpendicular fracture sets is lower than that for a model with randomly oriented fractures. Also, the truncation of the distribution of fracture lengths impacts the threshold value. Since the percolation threshold value is not our focus, here we consider 0.5 to 0.7 as a reasonable value of percolation threshold. For the cases we study here, the value of the percolation parameter p of initial fracture network is around 0.9. For the definition of p in Eq. (4), a value p = 1 corresponds to infinite fracture density

(zero probability of not intersecting another fracture). Thus our facture network is far above the percolation threshold and is well-connected, as one can see in the figures below.

3. IDENTIFYING THE CRITICAL SUB-NETWORK BASED ON FLOW SIMULATION RESULTS

3.1 Models without correlation between fracture aperture and length

3.1.1 Power-law aperture distribution

Some field observations and experimental studies show that a power-law distribution describes the fracture aperture distribution, although the available data is limited, especially from subsurface populations [44-49]. The power-law aperture distribution is described by Eq. (1). Previous studies find that the value of the exponent of the power-law aperture distribution in nature α is 1, 1.1, 1.8, 2.2, or 2.8. To include the entire range of feasible cases, here we study α in the range from 1 to 6. In each case, fracture aperture is limited to the interval between 0.01 mm and 10 mm. Because of this truncation, as the exponent α increases from 1 to 6, the fracture apertures concentrate in a narrow range near the lower limit (Fig. 2). For α = 1, apertures lie mostly in the range of 0.01 mm to 10 mm: the difference between smallest and largest value is nearly three orders of magnitude. For α = 4 to 6, most apertures lie between 0.01 mm and 0.03 mm. Absolute aperture is not important in the dimensionless results to follow, but a narrow range of apertures does affect the results.

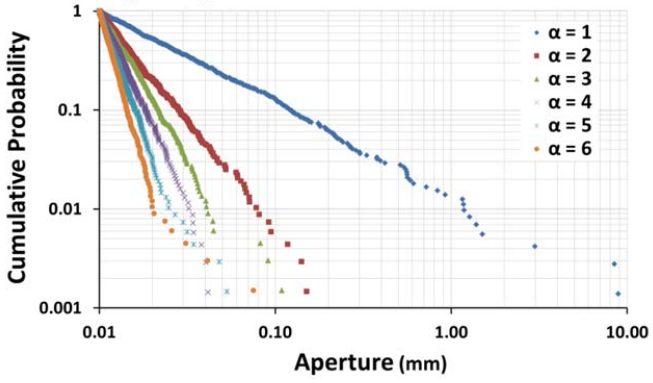

Figure 2 Fracture aperture follows a power-law distribution with different values of the exponent.

After running flow simulations on the percolation cluster of the original fracture network, we determine the value of $Q_{average}$ for each fracture. The fractures with the smallest $Q_{average}$ are eliminated first, then the larger ones. Numerical simulations presented in Fig. 3 show that when power-law aperture distribution exponent α = 1, approximate 60% of fractures can be eliminated, while retaining 90% of the network equivalent permeability. We call this sub-network retaining 90% of the original equivalent permeability the critical sub-network. As exponent α increases from 1 to 6, fewer and fewer fractures can be removed without significantly reducing the network equivalent permeability. In the case of α = 6, only 30% fractures can be eliminated while retaining 90% of the original equivalent permeability.

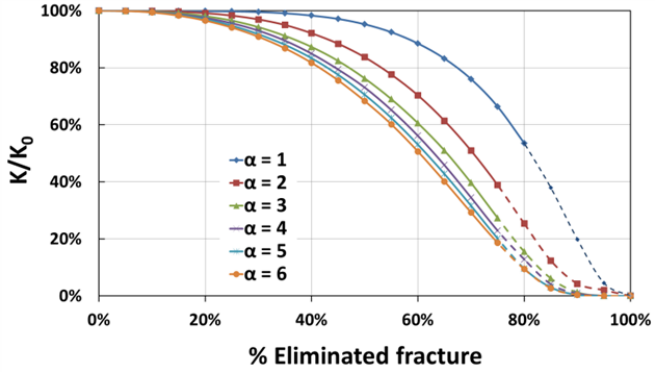

Figure 3 Sub-network equivalent permeability (K) normalized by the equivalent permeability of original fracture network (K_0), plotted against percent eliminated fractures, for a power-law aperture distribution with exponent α = 1 to 6. Each plotted point is the average value of 100 realizations generated with the given parameter values. A dashed line means that after the given portion of fractures is eliminated there is no percolating cluster left in at least some of the realizations.

In the network, some subset of fractures do not participate in fluid flow; these are known as dead-end or dangling fractures. To identify the flow structure in fracture networks, the backbone of original fracture network and sub-network are determined by removing fractures which do not belong to the spanning cluster, as well as dead-ends (Fig. 4). As shown in Fig. 4, the structure of the sub-network that retains 90% of original equivalent network permeability depends on α. For α = 1 (Fig. 4b), the backbone is much more sparse than that for others, because many more fractures can be removed without reducing permeability greatly.

The importance of fractures to fluid flow is not simply related to fracture length or fracture aperture. Figure 5 shows that when fractures are deleted according to flow-simulation results, the backbone length of each sub-network decreases almost linearly. This shows, for instance, that it is not exclusively short fractures that are eliminated first. The trend is nearly the same for different values of α. The length L is the cumulative length of all fracture segments in the backbone, not the length of all fractures with some segment in the backbone. Thus for the original network the reduction in length by about 20% arises mostly from eliminating segments, not whole fractures.

Figure 6 shows the standard deviation of apertures in the backbone after deletion of the fractures least-important to flow. The overall trend is for increasing standard deviation as more fractures are removed, until some sub-networks are disconnected entirely (dashed lines in Fig. 6). (These cases are counted as having zero standard

deviation; hence the decrease in the average standard deviation for the group.) For α = 1, when the first fractures are removed, the standard deviation in aperture in the backbone decreases at first, and then follows the trend for α = 2 to 6. Interpreting this plot in terms of aperture distribution is tricky. If narrower fractures were systematically eliminated, the standard deviation in aperture in the remaining fractures would increase modestly, but in a way that depends strongly on α. In Fig. 6, there is no clear trend with α.

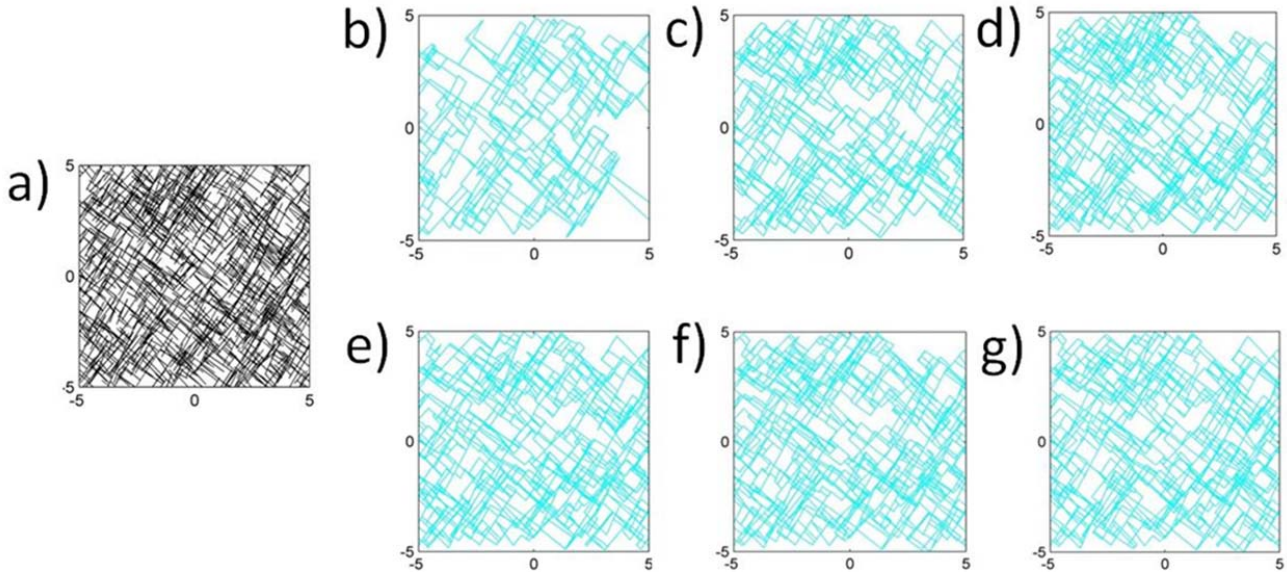

Figure 4 Original fracture network and backbone of the sub-network which retain 90% original equivalent network permeability: (a) original fracture network. (b)-(g) sub-network which retain 90% of network permeability: (b) α = 1, (c) α = 2, (d) α = 3, (e) α = 4, (f) α = 5, (g) α = 6.

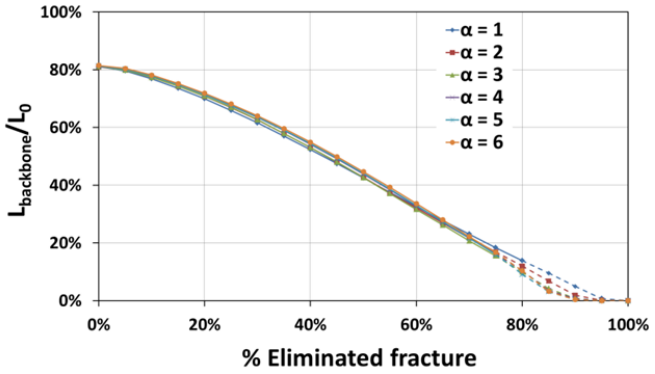

Figure 5 Length of sub-network backbone ($L_{backbone}$) normalized by the total length of original fracture network (L_0) plotted against percentage of eliminated fractures, for a power-law aperture distribution with exponent α = 1 to 6.

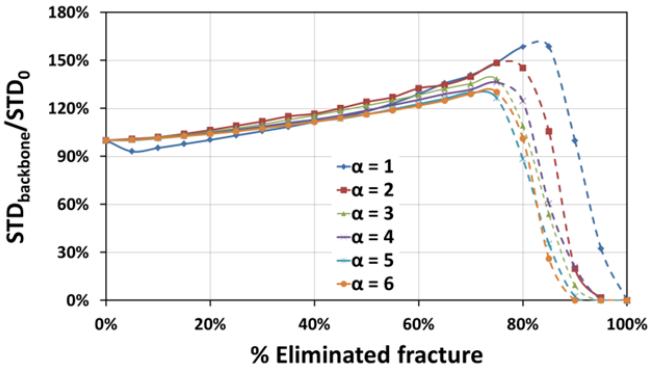

Figure 6 Standard deviation of apertures in sub-network backbone ($STD_{backbone}$) normalized by the standard deviation of apertures in original fracture network (STD_0), plotted against percentage of eliminated fractures, for power-law aperture distribution with exponent α = 1 to 6.

Figure 7 plots the minimum aperture in the backbone against the percentage of fractures removed. This minimum aperture in the backbone remains quite close to the minimum aperture of original fracture network until 70% fractures are removed. For α = 1, the ratio increases between 60% and 80% of fractures removed, but only by 50%. This demonstrates that there exist at least some fractures whose aperture is relatively narrow, that play a more important role in overall flow than others with larger aperture.

Figure 8 presents the average fracture aperture in the backbone after removing fractures which conduct the least flow. For all the cases, the average aperture increases as more fractures are removed, until there are no spanning cluster in some sub-networks (dashed lines in Fig. 8). The greatest change is in the cases where α = 1: the ratio increases by 250% when 80% of fractures are eliminated. Considering the difference between the smallest aperture and the largest aperture is three orders of magnitude, the average aperture in the sub-network backbone does not increase greatly. For α = 2 to 6, the average value changes only slightly. This indicates that

the fractures with small aperture are not systematically removed.

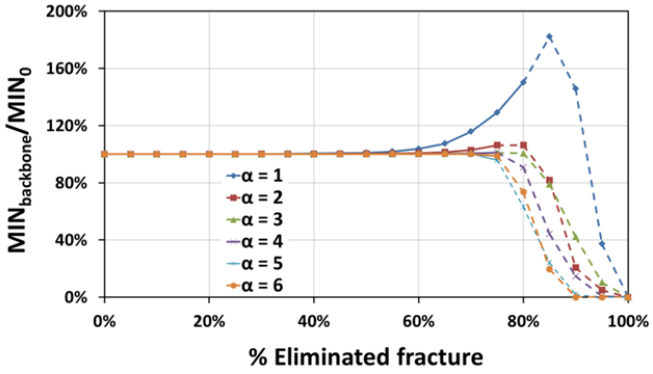

Figure 7 Minimum aperture of sub-network backbone ($MIN_{backbone}$) normalized by the minimum aperture of original fracture network (MIN_0), plotted against percentage of eliminated fracture, for power-law aperture distributions with exponent α = 1 to 6.

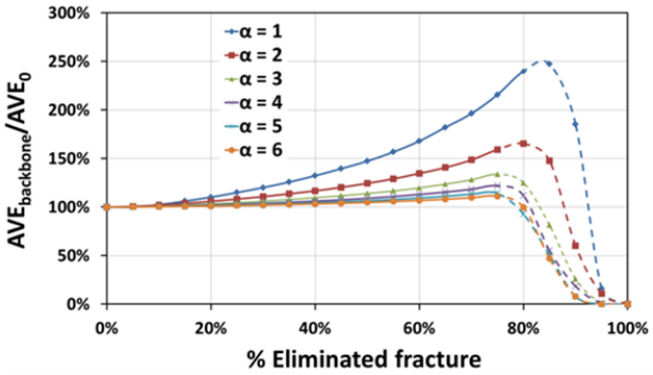

Figure 8 Average aperture of sub-network backbone ($AVE_{backbone}$) normalized by the average aperture of original fracture network (AVE_0), plotted against percentage of eliminated fractures, for power-law aperture distributions with exponent α = 1 to 6.

3.1.2 *Log-normal aperture distribution*

Some researchers propose a log-normal distribution of apertures based on field studies and hydraulic tests [7, 8, 51-54]. Fracture-network models with log-normal distributions of apertures have been widely used to simulate experiments and derive theoretical relationships [7, 8, 23, 27, 28, 50-53]. The log-normal distribution is specified by the following probability density function:

$$f(x) = \frac{1}{x \ln 10\, \sigma\sqrt{2\pi}} exp\left\{-\frac{1}{2}\left(\frac{\log_{10}(x)-\mu}{\sigma}\right)^2\right\} \quad (6)$$

where μ and σ are the mean and standard deviation in log-10 space. The truncated log-normal distribution has two additional parameters: a minimum and a maximum value, which are 0.01 mm and 10 mm, respectively. For the standard deviation, field studies and hydraulic tests found values of σ from 0.1 to 0.3, 0.23, and 0.47 [52-54]. To test the widest range of feasible values, we test values of σ from 0.1 to 0.6, as illustrated in Fig. 9.

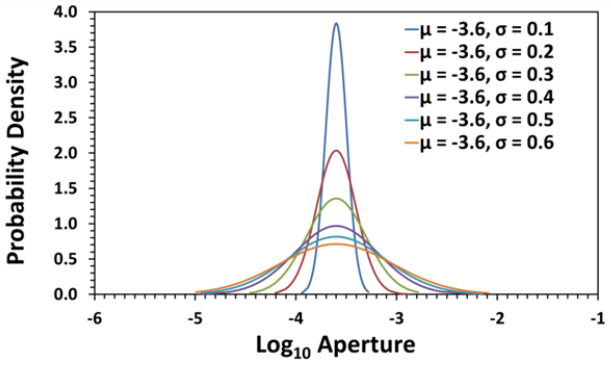

Figure 9 Fracture aperture follows log-normal distribution with the same mean value but different standard deviation in log-10 space.

Similar to our approach with the power-law aperture distributions, first we run flow simulations for each realization, and then eliminate fractures based on the flow simulation results, starting with fractures with the smallest $Q_{average}$. For each sub-network, the equivalent permeability is calculated. The average values are calculated over the 100 realizations for each set of parameter values (Fig. 10). The broader the aperture distribution is, the more fractures can be removed from the system while retaining a given fraction of the original network permeability. For example, to retain 90% of original network equivalent permeability, around 32% of fractures can be removed for the case of σ = 0.1 and more than 75% for σ = 0.6.

Clearly, the critical sub-network which retains 90% of the original equivalent permeability is strongly affected by the aperture distribution.

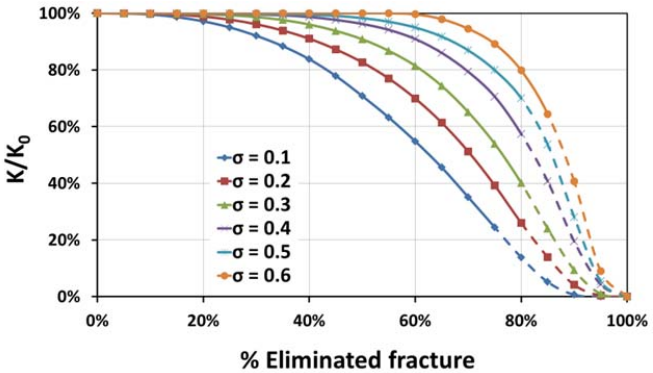

Figure 10 Sub-network equivalent permeability (K) normalized by the equivalent permeability of original fracture network (K_0), plotted against percentage of eliminated fractures, for log-normal aperture distributions with same log-mean value but log-standard deviations (σ) from 0.1 to 0.6.

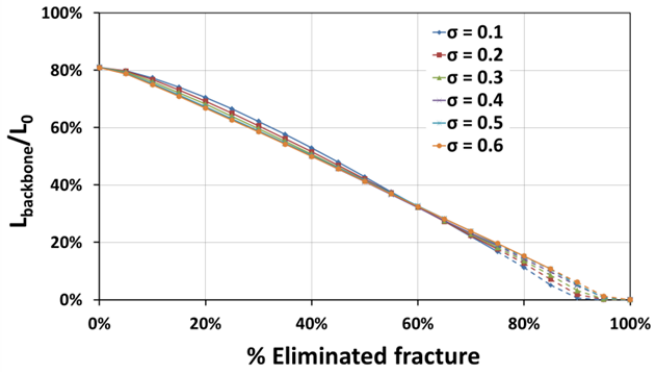

Figure 11 Length of sub-network backbone ($L_{backbone}$) normalized by the total length of original fracture network (L_0) plotted against percentage of eliminated fractures, for log-normal aperture distributions with same log-mean value but log-standard deviations (σ) from 0.1 to 0.6.

Similar to the case of a power-law aperture distribution, the length of the backbone for sub-networks decreases nearly linearly with increasing portion of fractures eliminated based on the flow simulation results. As presented in Fig. 11, the length of the backbone for the original fracture network is around 80% of total fracture length, regardless of the value of σ. As in Fig. 4, the ratio shown in Fig. 11 starts at about 0.8 for zero fractures removed because not all fracture segments in the original network are on the backbone.

Similar to the case of a power-law aperture distribution, the standard deviation of apertures in the sub-network (Fig. 12) does not change greatly as fractures are eliminated. For the cases σ = 0.1 and σ = 0.2, the aperture distribution becomes slightly narrower, and, for the rest of the cases, the aperture distribution of the sub-network becomes somewhat broader (Fig. 12).

The minimum aperture of the sub-network (Fig. 13) behaves differently from that for the cases of a power-law aperture distribution (cf. Fig. 5). The narrowest aperture in the network increases greatly as more fractures are eliminated. This suggests that the fractures with smaller aperture are eliminated preferentially. Another possible reason for the difference with cases with the power-law distribution is that there are relatively few very small apertures in log-normal distribution (Fig. 8), while by far most apertures have similar, small values for the power-law distributions (Fig. 1).

The average fracture aperture of the sub-network (Fig. 14) shows similar behavior to the cases of a power-law aperture distribution. The overall trend is that the average aperture increases as fractures are eliminated. When a certain percentage of fractures are removed (e.g. 60%), the average aperture of the sub-network becomes larger as σ increases from 0.1 to 0.6. The reason could be that the apertures distribute more broadly, and the difference between apertures is larger, with a larger σ.

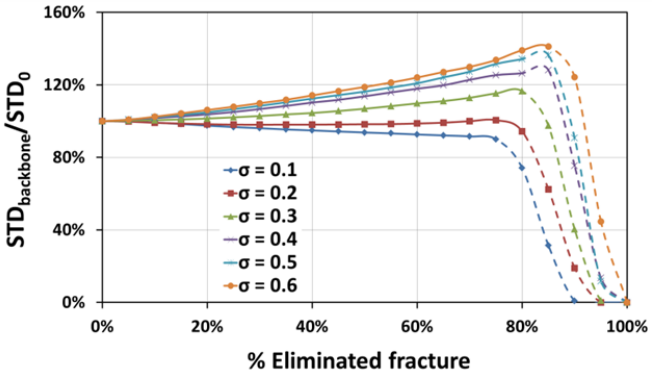

Figure 12 Standard deviation of apertures in sub-network backbone ($STD_{backbone}$) normalized by the standard deviation of apertures in original fracture network (STD_0), plotted against percentage of eliminated fractures, for log-normal aperture distributions with same log-mean value but log-standard deviations (σ) from 0.1 to 0.6.

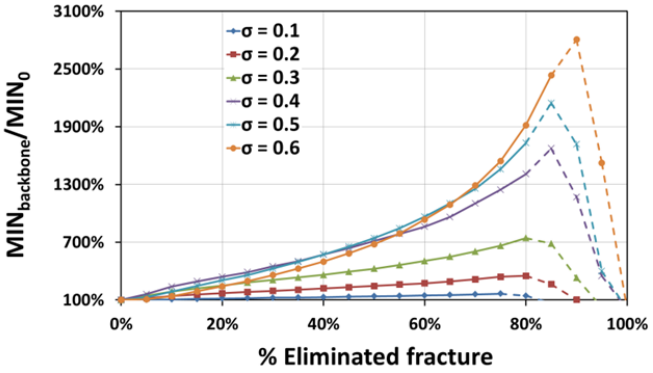

Figure 13 Minimum aperture of sub-network backbone ($MIN_{backbone}$) normalized by the minimum aperture of original fracture network (MIN_0), plotted against percentage of eliminated fractures, for log-normal aperture distributions with same log-mean value but log-standard deviations (σ) from 0.1 to 0.6.

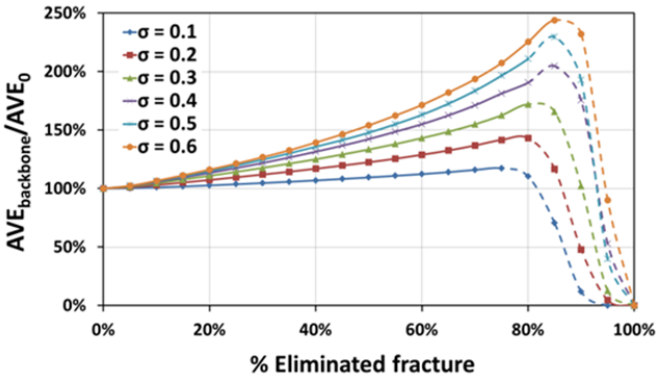

Figure 14 Average aperture of fracture in sub-network backbone ($AVE_{backbone}$) normalized by the average aperture of original fracture network (AVE_0), plotted against percentage of eliminated fractures, for log-normal aperture distributions with same log-mean value but log-standard deviations (σ) from 0.1 to 0.6.

3.2 Aperture linearly related to fracture length

Field measurements and theoretical studies raise the possibility of a relationship between fracture aperture and fracture length [55-59]. Both nonlinear and linear

relationships have been proposed in previous studies based on elastic theory and field data. Here we assume that the aperture of each fracture is uniform and linearly correlated with fracture length:

$$A = CL \quad (7)$$

where A is aperture, C is an empirical coefficient, and L is fracture length. Vermilye and Scholz [57] suggest the empirical coefficient lies between 1×10^{-3} and 8×10^{-3}. Here for the Mafic™ calculations we use 2×10^{-3}, but, since we normalize by the properties of the original fracture network, the value of C is unimportant to what follows. As mentioned above, all the cases we tested in this study have a power-law length distribution with exponent α = 2, truncated between 0.6 m and 6 m. Since aperture is proportional to fracture length, the apertures also follow a power-law distribution with exponent α = 2, in the range of 1.2 mm to 12 mm. As presented in Fig. 15, for the case described above with α = 2 and aperture independent of fracture length, the apertures lie mostly in the range of 0.01 mm to 0.1 mm: the difference between smallest and largest value is nearly one order of magnitude. When aperture is linearly related to fracture length, the apertures lie between 1.2 mm and 10 mm. Although the absolute values are different, the difference between smallest and largest value in both cases is similar: nearly one order of magnitude. The difference in magnitude of apertures between the two models is not important to what follows, but the truncation of the distribution at the largest values could have some effect.

Similar to the cases where apertures are independent of fracture length, first we run flow simulations for each realization, and determine the value of $Q_{average}$ for each fracture. Then we eliminate fractures, starting with those with the smallest $Q_{average}$. Figure 16 shows the sub-network equivalent permeability plotted against percent eliminated fractures for both cases, where aperture is independent of, and linearly related to, fracture length. The sub-network equivalent permeability behaves similarly for the two cases. Approximately 50% of fractures can be eliminated while retaining 90% of the network equivalent permeability.

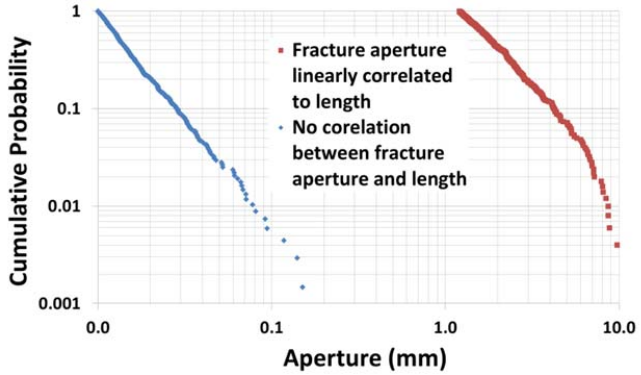

Figure 15 Fracture aperture follows power-law distribution with and without correlation to length (α = 2).

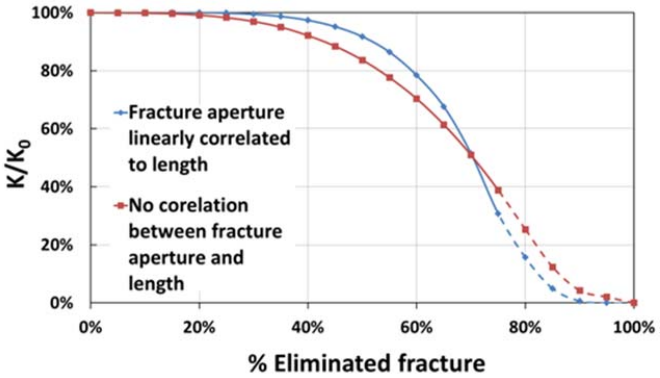

Figure 16 Sub-network equivalent permeability (K) normalized by the equivalent permeability of original fracture network (K_0), plotted against percent eliminated fractures, for the cases where aperture is independent of or proportional to fracture length, respectively.

Figure 17 shows the cumulative length of the sub-network backbone for the two cases. The cumulative length of the sub-network backbone decrease almost linearly until around 70% of fractures are removed, when there is no spanning cluster in at least some cases. Similar to the case where aperture is independent of fracture length, for the case where aperture is linearly related to length, the standard deviation of apertures in the sub-network (Fig.18) does not change greatly as fractures are eliminated.

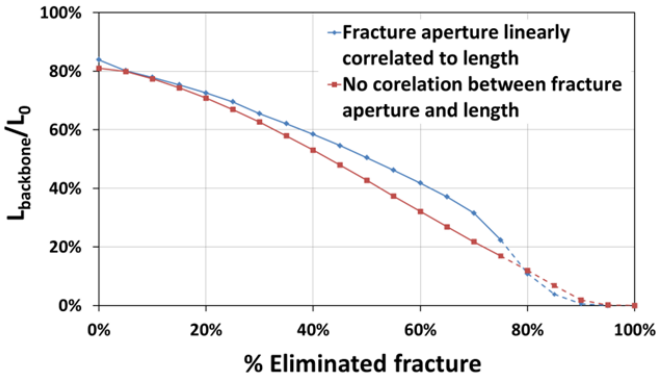

Figure 17 Length of sub-network backbone ($L_{backbone}$) normalized by the total length of original fracture network (L_0), plotted against percentage of eliminated fractures, for the cases where aperture is independent of or proportional to fracture length, respectively.

The minimum aperture of the sub-network (Fig. 19) behaves differently from that for the cases with no correlation between aperture and fracture length cases. When 70% of fractures are removed, the narrowest aperture in the sub-network is three times the value of the initial fracture network. Considering that the difference between the smallest and largest aperture is only one order of magnitude when α = 2 (Fig. 15), the minimum aperture of the sub-network increases greatly. This suggests that the fractures with smaller aperture are eliminated first.

Fig. 20 shows the average aperture in the sub-network. For both of the cases, the ratio between average aperture

of the sub-network and that of initial fracture network increases as more fractures are eliminated.

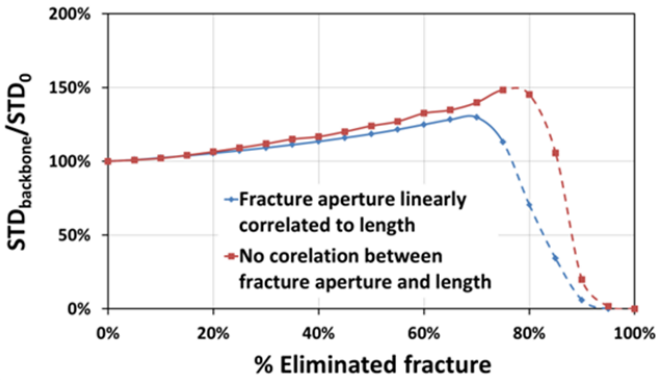

Figure 18 Standard deviation of apertures in sub-network backbone ($STD_{backbone}$) normalized by the standard deviation of apertures in original fracture network (STD_0), plotted against percentage of eliminated fractures, for the cases where aperture is independent of or proportional to fracture length, respectively.

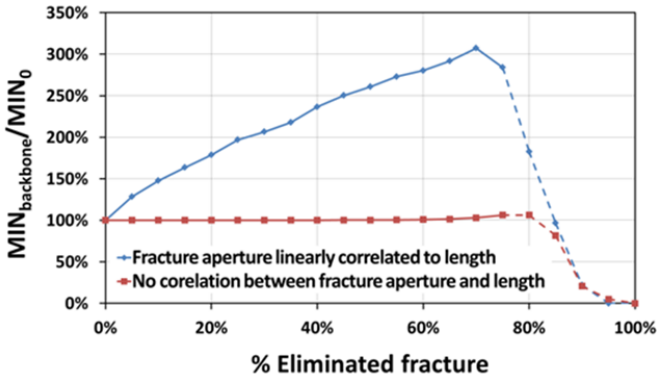

Figure 19 Minimum aperture in sub-network backbone ($MIN_{backbone}$) normalized by the minimum aperture in original fracture network (STD_0), plotted against percentage of eliminated fractures, for the cases where aperture is independent of or proportional to fracture length, respectively.

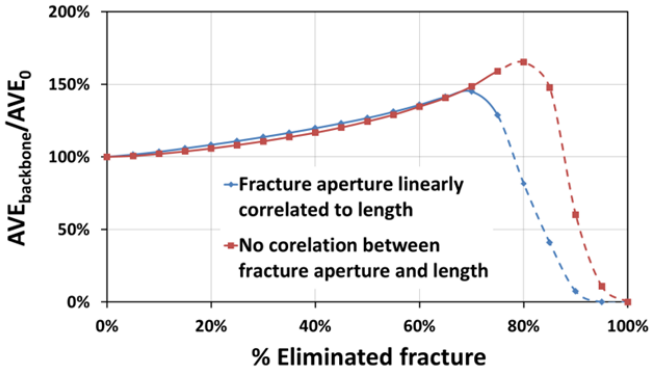

Figure 20 Average aperture in sub-network backbone ($AVE_{backbone}$) normalized by the average aperture in original fracture network (AVE_0), plotted against percentage of eliminated fractures, for the cases where aperture is independent of or proportional to fracture length, respectively.

4. POSSIBILITY OF IDENTIFYING CRITICAL SUB-NETWORK WITHOUT DOING FLOW SIMULATIONS

In section 3 we show that when the aperture distribution is broad enough, most fractures can be eliminated without significantly affecting the effective permeability. The fractures are eliminated based on the value of $Q_{average}$, which is obtained from flow simulations. We would like to explore a criterion for obtaining a sparse critical sub-network without doing flow simulations. The results in section 3 clearly show that aperture distribution has a strong influence on the critical sub-network. Also, the fracture length has an important impact on the flow behavior of fracture networks. Besides aperture and length, the other factor we consider here is the number of intersections each fracture has with other fractures. It is believed that this term reflects the importance of a fracture to the connectivity of the fracture network (hence the proposed percolation parameter for fracture networks based on intersections per fracture, mentioned above). We define criteria that are a combination of these three factors.

Table.1 Fracture-Elimination Criteria

Criterion	Description
1	Aperture (A)
2	Length (L)
3	Aperture × Length (A × L)
4	Aperture × Length × Number of intersections (A × L × N)
5	Flow simulation results (Q)

We compare the effective permeability of the sub-network with a portion of fractures eliminated using these criteria. Not all the cases examined above are studied here. For cases with a power-law aperture distribution, we study α = 1, 2, and 6. For cases of log-normal aperture distribution, we examine σ = 0.1, 0.2, and 0.6. We also test the case where aperture is linearly related to fracture length.

As presented in Figs. 20 to 26, if we consider the sub-network which can retain 90% of the effective permeability as a good approximation of the total fracture network, we can eliminate the most fractures using the flow simulation results. Next to that, in general, [Aperture × Length] is a better choice than the others (more fractures can be eliminated). For the case in which aperture is proportional to fracture length, the results obtained according to criteria 1 to 3 are the same. Thus, only three plots are shown in Fig. 26. Remarkably, when fractures are eliminated according to fracture length, the effective permeability of sub-network changes nearly linearly in all the cases.

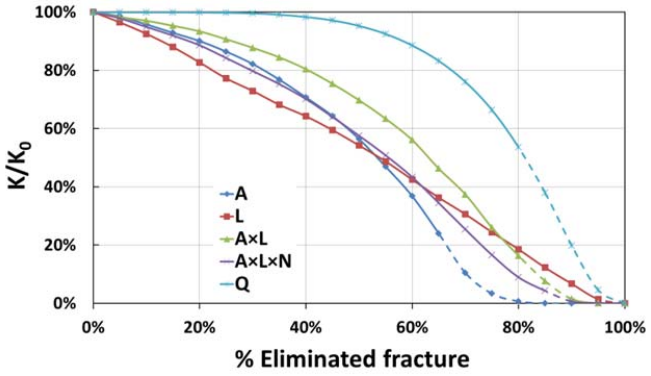

Figure 21 Sub-network equivalent permeability (K) normalized by the equivalent permeability of original fracture network (K_0), plotted against percent eliminated fractures, for a power-law aperture distribution with exponent $\alpha = 1$. Fractures are eliminated according to different criteria.

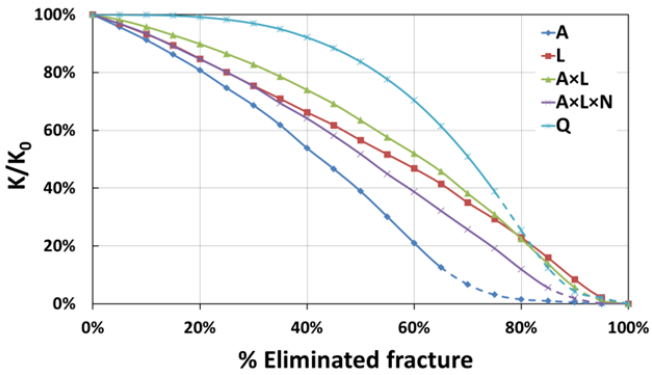

Figure 22 Sub-network equivalent permeability (K) normalized by the equivalent permeability of original fracture network (K_0), plotted against percent eliminated fractures, for a power-law aperture distribution with exponent $\alpha = 2$. Fractures are eliminated according to different criteria.

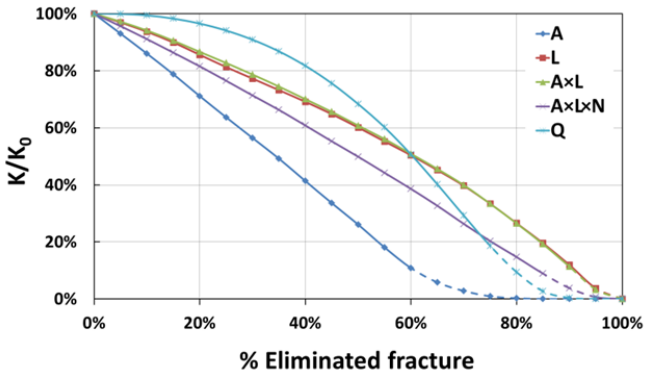

Figure 23 Sub-network equivalent permeability (K) normalized by the equivalent permeability of original fracture network (K_0), plotted against percent eliminated fractures, for a power-law aperture distribution with exponent $\alpha = 6$. Fractures are eliminated according to different criteria.

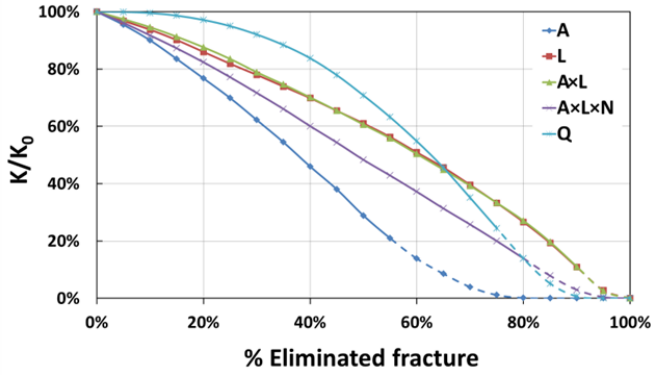

Figure 24 Sub-network equivalent permeability (K) normalized by the equivalent permeability of original fracture network (K_0), plotted against percentage of eliminated fractures, for log-normal aperture distributions with log-standard deviation $\sigma = 0.1$. Fractures are eliminated according to different criteria.

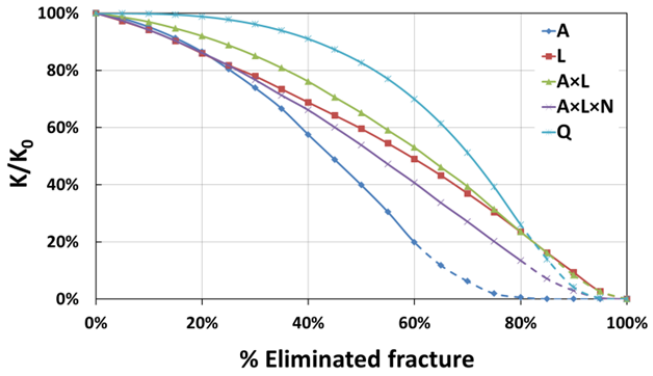

Figure 25 Sub-network equivalent permeability (K) normalized by the equivalent permeability of original fracture network (K_0), plotted against percentage of eliminated fractures, for log-normal aperture distributions with log-standard deviation $\sigma = 0.2$. Fractures are eliminated according to different criteria.

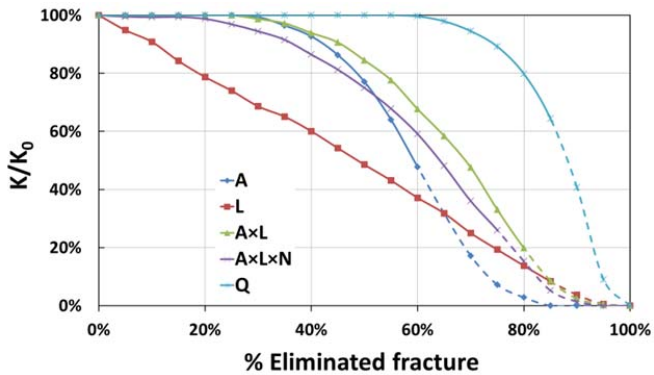

Figure 26 Sub-network equivalent permeability (K) normalized by the equivalent permeability of original fracture network (K_0), plotted against percentage of eliminated fractures, for log-normal aperture distributions with log-standard deviation $\sigma = 0.6$. Fractures are eliminated according to different criteria.

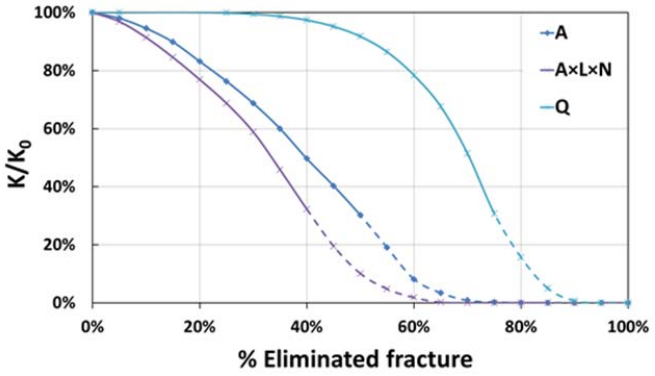

Figure 27 Sub-network equivalent permeability (K) normalized by the equivalent permeability of original fracture network (K_0), plotted against percentage of eliminated fractures, for case where aperture is linearly related to fracture length. Fractures are eliminated according to different criteria.

5. CONCLUSIONS

This work focuses on the effect of aperture distribution on the critical sub-network and its properties. A number of cases are tested: narrow and broad log-normal and power-law distributions, and one where aperture correlates with fracture length. Several following conclusions reflect the strong influence of aperture distribution on flow behavior.

- For the fracture networks with power-law or log-normal aperture distributions, or aperture proportional to fracture length, if the aperture distribution is broad enough, most of fractures can be eliminated without significantly affecting the effective permeability. This is true even though the original fracture network is well-connected.
- As the exponent α of a power-law aperture distribution increases or the standard deviation σ of a log-normal aperture distribution decreases, fewer and fewer fractures can be removed without significantly reducing the network equivalent permeability. The critical sub-network for flow is strongly affected by the aperture distribution.
- For all the cases, when the fractures are removed according to the flow-simulation results, the cumulative length of sub-network backbone decreases nearly linearly as more fractures are eliminated.
- For the cases of power-law aperture distribution, there exist at least some fractures whose aperture is relatively narrow that play a more important role in overall flow than some others with larger aperture.
- For the cases of log-normal aperture distribution, the standard deviation of apertures in the backbone and the average aperture in the sub-network backbone behaves similarly to the cases with a power-law aperture distribution. But the narrowest aperture in the network increases greatly as more fractures are eliminated, in contrast to behavior with a power-law aperture distribution.
- For the cases where aperture is independent of fracture length and aperture is correlated to fracture length with the same power-law aperture-distribution exponent $\alpha = 2$, the behavior of the effective sub-network permeability, the cumulative length of sub-network backbone, the standard deviation of apertures and the average aperture in the sub-network backbone are similar to each other. But the narrowest aperture in the sub-network increase significantly for the case where aperture is correlated to fracture length, which is different from the cases where aperture is independent of fracture length.
- If we consider the sub-network which can retain 90% of the effective permeability as a good approximation of the total fracture network, we can eliminate the most fractures using the flow simulation results. Besides that, in general, [Aperture × Length] is a better choice for obtaining a sparse critical sub-network than the others considered here.

REFERENCES

1. Saidi, A.M., *Reservoir engineering of fractured reservoirs (fundamental and practical aspects)*. 1987, Paris: Total Edition Press.
2. Aguilera, R., *Naturally fractured reservoirs*. 1980: Petroleum Publishing Company.
3. van Golf-Racht, T.D., *Fundamentals of fractured reservoir engineering*. 1982: Elsevier.
4. Neretnieks, I., T. Eriksen, and P. Tähtinen, *Tracer movement in a single fissure in granitic rock: Some experimental results and their interpretation.* Water Resources Research, 1982. **18**(4): p. 849-858.
5. Neretnieks, I., *Solute transport in fractured rock: applications to radionuclide waste repositories.* Flow and contaminant transport in fractured rock, 1993: p. 39-127.
6. Tsang, C.F. and I. Neretnieks, *Flow channeling in heterogeneous fractured rocks.* Reviews of Geophysics, 1998. **36**(2): p. 275-298.
7. Cacas, M., et al., *Modeling fracture flow with a stochastic discrete fracture network: Calibration and validation: 1. The flow model.* Water Resources Research, 1990. **26**(3): p. 479-489.
8. Cacas, M., et al., *Modeling Fracture Flow With a Stochastic Discrete Fracture Network: Calibration and Validation 2. The Transport Model.* Water Resources Research, 1990. **26**: p. 491-500.
9. Schwartz, F.W., L. Smith, and A.S. Crowe, *A stochastic analysis of macroscopic dispersion in fractured media.* Water Resources Research, 1983. **19**(5): p. 1253-1265.
10. Englman, R., Y. Gur, and Z. Jaeger, *Fluid flow through a crack network in rocks.* Journal of applied mechanics, 1983. **50**(4a): p. 707-711.
11. Robinson, P., *Connectivity of fracture systems-a percolation theory approach.* Journal of Physics A: Mathematical and General, 1983. **16**(3): p. 605.

12. Robinson, P., *Numerical calculations of critical densities for lines and planes.* Journal of Physics A: Mathematical and General, 1984. **17**(14): p. 2823.
13. Smith, L. and F.W. Schwartz, *An analysis of the influence of fracture geometry on mass transport in fractured media.* Water Resources Research, 1984. **20**(9): p. 1241-1252.
14. Andersson, J. and B. Dverstorp, *Conditional simulations of fluid flow in three ‐ dimensional networks of discrete fractures.* Water Resources Research, 1987. **23**(10): p. 1876-1886.
15. Hestir, K. and J. Long, *Analytical expressions for the permeability of random two ‐ dimensional Poisson fracture networks based on regular lattice percolation and equivalent media theories.* Journal of Geophysical Research: Solid Earth (1978–2012), 1990. **95**(B13): p. 21565-21581.
16. Balberg, I., B. Berkowitz, and G. Drachsler, *Application of a percolation model to flow in fractured hard rocks.* Journal of Geophysical Research: Solid Earth (1978–2012), 1991. **96**(B6): p. 10015-10021.
17. Berkowitz, B. and I. Balberg, *Percolation theory and its application to groundwater hydrology.* Water Resources Research, 1993. **29**(4): p. 775-794.
18. David, C., *Geometry of flow paths for fluid transport in rocks.* Journal of Geophysical Research: Solid Earth (1978–2012), 1993. **98**(B7): p. 12267-12278.
19. Berkowitz, B., *Analysis of fracture network connectivity using percolation theory.* Mathematical Geology, 1995. **27**(4): p. 467-483.
20. Berkowitz, B. and H. Scher, *Anomalous transport in random fracture networks.* Physical review letters, 1997. **79**(20): p. 4038.
21. Berkowitz, B. and H. Scher, *Theory of anomalous chemical transport in random fracture networks.* Physical Review E, 1998. **57**(5): p. 5858.
22. Dreuzy, J.R., P. Davy, and O. Bour, *Hydraulic properties of two ‐ dimensional random fracture networks following a power law length distribution: 1. Effective connectivity.* Water Resources Research, 2001. **37**(8): p. 2065-2078.
23. Charlaix, E., E. Guyon, and S. Roux, *Permeability of a random array of fractures of widely varying apertures.* Transport in porous media, 1987. **2**(1): p. 31-43.
24. Tsang, Y.W. and C. Tsang, *Channel model of flow through fractured media.* Water Resources Research, 1987. **23**(3): p. 467-479.
25. Tsang, Y., et al., *Flow and tracer transport in fractured media: A variable aperture channel model and its properties.* Water Resources Research, 1988. **24**(12): p. 2049-2060.
26. Nordqvist, A.W., et al., *Effects of high variance of fracture transmissivity on transport and sorption at different scales in a discrete model for fractured rocks.* Journal of contaminant hydrology, 1996. **22**(1): p. 39-66.
27. Margolin, G., B. Berkowitz, and H. Scher, *Structure, flow, and generalized conductivity scaling in fracture networks.* Water Resources Research, 1998. **34**(9): p. 2103-2121.
28. de Dreuzy, J.-R., P. Davy, and O. Bour, *Hydraulic properties of two-dimensional random fracture networks following a power law length distribution: 2. Permeability of networks based on lognormal distribution of apertures.* Water Resources Research, 2001. **37**: p. 2079-2095.
29. de Dreuzy, J.R., P. Davy, and O. Bour, *Hydraulic properties of two ‐ dimensional random fracture networks following power law distributions of length and aperture.* Water Resources Research, 2002. **38**(12): p. 12-1-12-9.
30. de Dreuzy, J.-R., P. Davy, and O. Bour, *Hydraulic properties of two-dimensional random fracture networks following a power law length distribution: 1. Effective connectivity.* Water Resources Research, 2001. **37**(8): p. 2065-2078.
31. Katz, A. and A. Thompson, *Prediction of rock electrical conductivity from mercury injection measurements.* Journal of Geophysical Research: Solid Earth (1978–2012), 1987. **92**(B1): p. 599-607.
32. Berkowitz, B., *Characterizing flow and transport in fractured geological media: A review.* Advances in water resources, 2002. **25**(8): p. 861-884.
33. Dershowitz, W., Lee,G., Geier, J., Foxford, T., LaPointe, P., Thomas, A., *User Documentation for FracMan*. 2011, Seattle, Washington: Golder Associates Inc.
34. Segall, P. and D.D. Pollard, *Joint formation in granitic rock of the Sierra Nevada.* Geological Society of America Bulletin, 1983. **94**(5): p. 563-575.
35. Rouleau, A. and J. Gale. *Statistical characterization of the fracture system in the Stripa granite, Sweden*. in *International Journal of Rock Mechanics and Mining Sciences & Geomechanics Abstracts*. 1985. Elsevier.
36. Bour, O. and P. Davy, *Connectivity of random fault networks following a power law fault length distribution.* Water Resources Research, 1997. **33**(7): p. 1567-1583.
37. Nicol, A., et al., *Fault size distributions—are they really power-law?* Journal of Structural Geology, 1996. **18**(2): p. 191-197.
38. Odling, N.E., *Scaling and connectivity of joint systems in sandstones from western Norway.* Journal of Structural Geology, 1997. **19**(10): p. 1257-1271.
39. Aharony, A. and D. Stauffer, *Introduction to percolation theory*. 2003: Taylor & Francis.
40. Masihi, M., P.R. King, and P.R. Nurafza. *Fast estimation of performance parameters in fractured reservoirs using percolation theory*. in *SPE Europec/EAGE Annual Conference*. 2005. Society of Petroleum Engineers.
41. Masihi, M., P.R. King, and P.R. Nurafza, *Connectivity prediction in fractured reservoirs with variable fracture size: Analysis and validation.* SPE Journal, 2008. **13**(01): p. 88-98.
42. Balberg, I., et al., *Excluded volume and its relation to the onset of percolation.* Physical review B, 1984. **30**(7): p. 3933.
43. Belayneh, M., et al., *Prediction of vein connectivity using the percolation approach: model test with field*

data. Journal of Geophysics and Engineering, 2006. **3**(3): p. 219.
44. Barton, C.A. and M.D. Zoback, *Self‐similar distribution and properties of macroscopic fractures at depth in crystalline rock in the Cajon Pass Scientific Drill Hole.* Journal of Geophysical Research: Solid Earth (1978–2012), 1992. **97**(B4): p. 5181-5200.
45. Barton, C.C., et al., *Physical and Hydrologic-Flow Properties of Fractures Las Vegas, Nevada—Zion Canyon, Utah—Grand Canyon, Arizona—Yucca Mountain, Nevada July 20–24, 1989*. Vol. 385. 1989: American Geophysical Union.
46. Belfield, W. and J. Sovich. *Fracture statistics from horizontal wellbores*. in *SPE/CIM/CANMET International Conference on Recent Advances in Horizontal Well Applications*. 1994. Petroleum Society of Canada.
47. Marrett, R., *Aggregate properties of fracture populations.* Journal of Structural Geology, 1996. **18**(2): p. 169-178.
48. Ortega, O. and R. Marrett, *Prediction of macrofracture properties using microfracture information, Mesaverde Group sandstones, San Juan basin, New Mexico.* Journal of Structural Geology, 2000. **22**(5): p. 571-588.
49. Wong, T.F., J.T. Fredrich, and G.D. Gwanmesia, *Crack aperture statistics and pore space fractal geometry of Westerly granite and Rutland quartzite: Implications for an elastic contact model of rock compressibility.* Journal of Geophysical Research: Solid Earth (1978–2012), 1989. **94**(B8): p. 10267-10278.
50. Feng, S., B. Halperin, and P. Sen, *Transport properties of continuum systems near the percolation threshold.* Physical Review B, 1987. **35**(1): p. 197.
51. Long, J. and D.M. Billaux, *From field data to fracture network modeling: An example incorporating spatial structure.* Water Resources Research, 1987. **23**(7): p. 1201-1216.
52. Dverstorp, B. and J. Andersson, *Application of the discrete fracture network concept with field data: Possibilities of model calibration and validation.* Water Resources Research, 1989. **25**(3): p. 540-550.
53. Tsang, Y., et al., *Tracer transport in a stochastic continuum model of fractured media.* Water Resources Research, 1996. **32**(10): p. 3077-3092.
54. Snow, D.T., *The frequency and apertures of fractures in rock.* International Journal of Rock Mechanics and Mining Sciences & Geomechanics Abstracts, 1970. **7**(1): p. 23-40.
55. Stone, D. *Sub-surface fracture maps predicted from borehole data: An example from the Eye-Dashwa pluton, Atikokan, Canada*. in *International Journal of Rock Mechanics and Mining Sciences & Geomechanics Abstracts*. 1984. Elsevier.
56. Hatton, C., I. Main, and P. Meredith, *Non-universal scaling of fracture length and opening displacement.* Nature, 1994. **367**(6459): p. 160-162.
57. Vermilye, J.M. and C.H. Scholz, *Relation between vein length and aperture.* Journal of Structural Geology, 1995. **17**(3): p. 423-434.
58. Johnston, J. and K. McCaffrey, *Fractal geometries of vein systems and the variation of scalingrelationships with mechanism.* Journal of Structural Geology, 1996. **18**(2): p. 349-358.
59. Renshaw, C. and J. Park, *Effect of mechanical interactions on the scaling of fracture length and aperture.* 1997.